Published OnlineFirst December 8, 2009; DOI: 10.1158/1535-7163.MCT-09-0415
Published Online First on December 8, 2009 as 10.1158/1535-7163.MCT-09-0415

Tumor necrosis factor–related apoptosis-inducing ligand (TRAIL) and paclitaxel have cooperative *in vivo* effects against glioblastoma multiforme cells

Jay F. Dorsey,[1,2,3] Akiva Mintz,[1,4] Xiaobing Tian,[1,2,3] Melissa L. Dowling,[2,3] John P. Plastaras,[1,2,3] David T. Dicker,[1] Gary D. Kao,[2,3] and Wafik S. El-Deiry[1,3]

[1]Laboratory of Molecular Oncology and Cell Cycle Regulation, Departments of Medicine (Hematology/Oncology), Genetics, Pharmacology, the Institute for Translational Medicine and Therapeutics, [2]Department of Radiation Oncology, and [3]Radiation Biology and Imaging Program, Abramson Comprehensive Cancer Center, University of Pennsylvania School of Medicine, Philadelphia, Pennsylvania; and [4]Departments of Neurosurgery, Radiology, Radiation Oncology, Cancer Biology, and the Brain Tumor Center of Excellence, Wake Forest University School of Medicine, Winston-Salem, North Carolina

Abstract

Tumor necrosis factor–related apoptosis-inducing ligand (TRAIL) in conjunction with microtubule-targeting agents may be a promising novel anticancer treatment strategy. *In vitro* studies have suggested that relatively low concentrations of TRAIL enhance the lethality of paclitaxel (Taxol) against human cancer cells. The increased efficacy may be due to the triggering of caspase activation, resulting in mitotic checkpoint abrogation and catastrophe. We show here that wild-type p53 protects cells from caspase-dependent death induced by this therapeutic combination *in vitro*. We have now also developed an imaging-based model system to test the *in vivo* efficacy of combined TRAIL and Taxol, in which tumor growth and treatment response can be monitored noninvasively and in real-time. We further utilize bioluminescence, F^{18}-fluorodeoxyglucose-positron emission tomography, and microscale computed tomography imaging to confirm the effects of combined treatment on tumors. These studies together provide the first *in vivo* confirmation that combined TRAIL plus paclitaxel results in better tumor control compared with either TRAIL or paclitaxel alone, and with no discernable increased normal tissue toxicity in the mouse. Interestingly, the *in vivo* antitumor response elicited by combined treatment was not affected by the p53 status of the tumor cells. These preclinical observations together suggest the therapeutic potential of combining TRAIL plus paclitaxel in cancer treatment, and support further preclinical and future clinical testing. [Mol Cancer Ther 2009;8(12):3285–95]

Introduction

Glioblastoma multiforme (GBM) is the most common and aggressive primary malignant brain tumor in adults. Standard therapy for GBM consists of surgical resection followed by radiation therapy with concurrent and adjuvant temozolomide chemotherapy (1). Thus, standard therapy still only results in a median survival of ~14.6 months, and a progression-free survival of ~6.9 months; most patients eventually experience recurrences and die (1). Other chemotherapeutic agents have been investigated in the past for their efficacy against GBM with mixed results (2). A number of studies have investigated the efficacy of paclitaxel (Taxol) for treating GBM. Paclitaxel was investigated in a phase II study in GBM and found to be well tolerated (3). More recently, convection-enhanced delivery of paclitaxel for treatment of recurrent malignant glioma has been studied in a phase I/II clinical trial (4). Furthermore, newer formulations of paclitaxel are also being investigated preclinically for treatment of glioma, including Oncogel, a controlled-release depot formulation of paclitaxel that can be directly applied to local areas within the brain (5). Despite the interest in paclitaxel for treatment of GBM, antimicrotubule agents have not as of yet proven clinically useful as a single agent (3). New approaches including combination therapies are therefore urgently needed.

Tumor necrosis factor–related apoptosis-inducing ligand (TRAIL) is a potent cancer cell–specific apoptosis-inducing agent with little to no effect on normal tissues and, along with derivative agents, is being tested in early phase clinical trials (6),[5] with promising early results (7). However, TRAIL may ultimately prove to have greater efficacy when used in combination with traditional chemotherapy (8).

We recently reported our findings on the *in vitro* anticancer efficacy of TRAIL when combined with the microtubule-targeting drugs nocodazole and paclitaxel (9). Combined treatment

Received 5/11/09; revised 10/14/09; accepted 10/23/09; published OnlineFirst 12/8/09.

Grant support: Radiological Society of North America HPSD0609 (J.F. Dorsey), Burroughs Wellcome Fund Career Award for Medical Scientists 1006792 (J.F. Dorsey), and Public Health Service Grant P01 CA075138 (W.S. El-Deiry). W.S. El-Deiry is an American Cancer Society Research Professor.

The costs of publication of this article were defrayed in part by the payment of page charges. This article must therefore be hereby marked *advertisement* in accordance with 18 U.S.C. Section 1734 solely to indicate this fact.

Note: Supplementary material for this article is available at Molecular Cancer Therapeutics Online (http://mct.aacrjournals.org/).

Requests for reprints: Wafik S. El-Deiry, University of Pennsylvania School of Medicine, 415 Curie Boulevard, CRB 437A, Philadelphia, PA 19104. Phone: 215-898-9015; Fax: 215-573-9139. E-mail: wafik@mail.med.upenn.edu

doi:10.1158/1535-7163.MCT-09-0415

[5] http://www.clinicaltrials.gov

Published OnlineFirst December 8, 2009; DOI: 10.1158/1535-7163.MCT-09-0415

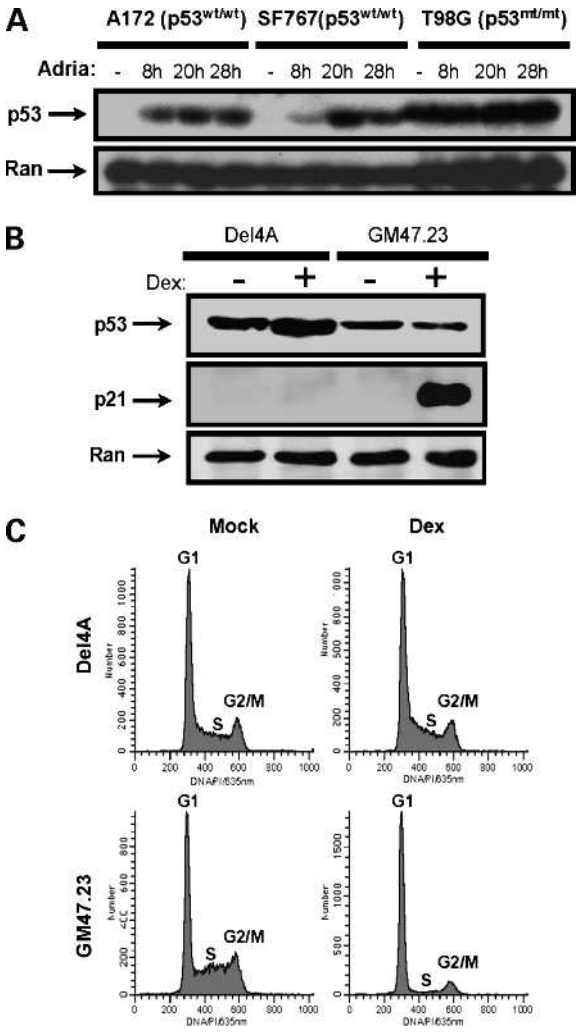

Figure 1. Wild-type p53 induction inhibits accumulation of glioma cells in M phase. **A,** A172, SF767, and T98G human glioma cells (1×10^6 cells) were plated, treated with Adriamycin (1 μg/mL), and harvested for Western blotting at the indicated times for analysis of p53 stabilization. **B,** T98G-derived cell lines Del4A and GM47.23 (1×10^6 cells) were mock induced or induced with Dexamethasone (*Dex*; 1 μmol/L) for 16 h and harvested for Western blotting of indicated proteins. **C,** Del4A and GM47.23 were mock induced or induced with Dexamethasone (1 μmol/L) overnight and harvested for flow cytometric analysis of DNA content using propidium iodide staining.

led to markedly greater caspase activation, and abrogation of the mitotic checkpoint than either TRAIL or microtubule-targeting alone, and caused significantly greater cancer cell death. In this work, we examined the effects of TRAIL alone, paclitaxel alone, or the combination of agents on GBM tumor xenografts. We present here the first preliminary report on the *in vivo* efficacy of TRAIL plus paclitaxel against human GBM xenografts using multimodality imaging including bioluminescence, microscale computed tomography (microCT), and positron emission tomography (PET). This work therefore confirms, in an *in vivo* GBM model system, our previously reported *in vitro* findings that combined TRAIL and paclitaxel treatment leads to maximal anticancer efficacy (9).

Materials and Methods

Reagents, Cell Lines, and *In vitro* Studies

SF767 and SF268 cell lines were obtained from the University of California at San Francisco/Brain Tumor Research Center Tissue Bank. T98G and A172 cell lines were obtained from the American Type Culture Collection. GM47.23 and Del4A cell lines were a gift from W. Edward Mercer (Thomas Jefferson University, Philadelphia, PA). All cell lines were maintained in RPMI + 10% fetal bovine serum, penicillin (100 U/mL), and streptomycin (100 mg/mL), and cultured at 37°C in humidified 5% CO_2. His-tagged TRAIL was prepared as previously described (10, 11). Dexamethasone and paclitaxel were obtained from Sigma-Aldrich. Caspase-glo 3/7 assay was done according to manufacturer's instructions (Promega). SF767 bioluminescent/biofluorescent cells were generated, verified for expression, and isolated as previously described (12).

Western Blotting

Western blot analysis of cell lysates were done as previously described (11). Immunoblotting was done with the following: rabbit anti–poly ADP ribose polymerase (PARP; 1:1,000), rabbit anti–phospho-bcl2 (1:1,000; Cell Signaling Technologies), mouse anti-FLIP (1:1,000), mouse anti-DR5 (1:1,000), rabbit anti–Mcl-1 (1:1,000), and mouse anti-Ran (1:5,000; BD Biosciences).

Xenograft Studies

All procedures involving the use of animals were conducted according to an Institutional Animal Care and Use Committee–approved protocol at the University of Pennsylvania. Nude mice (ages 4–6 wk) from Charles River laboratory were injected with 300 μL Matrigel (BD Collaborative Research) slurry (prepared at a 1:1 ratio with 1 × HBSS) containing 3 million cells. For *in vivo* treatment experiments, 20 mg/kg paclitaxel [solubilized in Cremophor EL (polyoxyethylated castor oil)/ethanol, 1:1 v/v formulation] or 100 μg of TRAIL was injected i.p. or via tail vein (i.v.), respectively, where indicated. Mock treatment consisted of 5 cc of saline injected i.p. or i.v.

Bioluminescence, Biofluorescence, F^{18}-Fluorodeoxyglucose-PET, and microCT Imaging

Bioluminescence. Nude mice were imaged using the Xenogen IVIS 2000 imaging platform, and data processing was conducted with Living Image Software (Caliper Life Sciences). The luciferase activity was measured by i.p. injection of 50 mg/mouse D-luciferin into anesthetized mice (i.p. ketamine/xylazine), followed by detection of live images using the Xenogen IVIS at 15 min postinjection. Regions of interest were drawn over the tumor areas as previously described (13, 14). Bioluminescence signal was recorded as maximum (photons/s/cm^2/steridian).

Biofluorescence. Nude mice were anesthetized (i.p. ketamine/xylazine) and then imaged using the Maestro *in vivo* imaging system with background autofluorescence correction (Cambridge Research and Instrumentation, Woburn, MA).

F^{18}-Fluorodeoxyglucose-PET and MicroCT. Tumor xenograft-bearing mice were injected with 0.5 mCi of F^{18}-fluorodeoxyglucose (FDG) in a volume of 0.2 mL saline via tail vein injection. Two hours postinjection, mice were secured

Published OnlineFirst December 8, 2009; DOI: 10.1158/1535-7163.MCT-09-0415

to a pallet with their body temperature maintained using a warming blanket and PET imaging was done on the A-PET small animal PET scanner at the University of Pennsylvania Small Animal Imaging Facility as previously described (15). Immediately following the PET scan, the animals were transferred to the microCat CT system for imaging as previously described (15). Image data were analyzed and reconstructed using Amira and Amide software. The tumors identified from microCT were manually segmented using Amira software to obtain the mean tumor volumes for each treatment cohort. Change in tumor volume (mm^3) was calculated as posttherapy volume measurement minus pretherapy volume measurement.

Statistical Analysis

Statistical differences were determined by Student's *t* test using the MedCalc (software version 10.4.8.0) statistical software package.

Results

Expression of Wild-Type p53 Attenuates Paclitaxel-Induced Mitotic Delay *In vitro*

We have proposed that TRAIL may increase the efficacy of chemotherapy invoking the mitotic checkpoint by augmenting caspase activation, which facilitates the degradation of spindle checkpoint proteins such as BubR1 and Bub1, resulting in abrogation of the cell cycle checkpoint (9). It has been suggested that activation of p53-dependent checkpoints may prevent cell death caused by microtubule-active drugs (16). Therefore, to better characterize the effect of p53 on cell cycle progression in response to treatment, as well as clarify the influence of p53 status on the efficacy of individual or combination treatments, we studied glioblastoma cell lines including those in which p53 expression was inducible.

T98G cells expressed a high baseline level of endogenous mutant p53 that is essentially unchanged by treatment with the DNA-damaging agent doxorubicin (Fig. 1A, *right*). In contrast, wild-type p53-expressing A172 (17) and SF767 (18), showed increased levels of endogenous p53 up to 28 hours after exposure to doxorubicin, consistent with the stabilization of wild-type p53 protein after exposure to DNA damage in these cell lines that normally express little detectable p53.

We next studied cell lines that were derived from but otherwise isogenic with T98G human GBM cells. Del4A cells were derived from T98G but have stably incorporated a vector expressing mutant p53 under the control of dexamethasone-responsive promoter (19). GM47.23 cells were also derived from T98G cells but have stably incorporated an expression vector in which wild-type p53 is driven by the same steroid-responsive promoter (20). Induction of mutant p53 in Del4A cells by dexamethasone (*Dex*) induced no detectable level of p21 protein (Fig. 1B, *middle row*). In contrast, induction of wild-type p53 in GM47.23 cells in turn led to robust increased expression of p21 and accumulation of GM47.23 cells in the G_1 phase of the cell cycle with a concomitant depletion of cells in the S- and G_2-M phase fractions (bottom panel of the fluorescence-activated cell sorting histograms shown in Fig. 1C; the induced wild-type p53 protein does not remain appreciably elevated over the high-background stable mutant p53 protein due to negative feedback that accelerates p53 degradation, but which does not prevent activation of downstream targets of p53 such as p21). On the other hand, induction of mutant p53 expression in Del4A cells by dexamethasone had no discernable effect on cell cycle distribution (Fig. 1C, *top*). By performing fluorescence-activated cell sorting analysis of phospho-histone H3 expression, we confirmed that p53 expression diminished the proportion of cells in M phase after paclitaxel treatment (Supplementary Fig. S2A and B).

Induced Expression of Wild-Type p53 Decreases *In vitro* Cell Death after Exposure to TRAIL and Paclitaxel

We previously showed that abrogation of the antimicrotubule-induced mitotic checkpoint by TRAIL leads to increased cancer cell death (9). We therefore sought to test whether the induced expression of wild-type p53 could potentially protect cells from the lethal effects of TRAIL on mitosis. Visual inspection by light microscopy suggested that Del4A and GM47.23 cells grown to confluence, but uninduced for protein, seemed largely unperturbed by paclitaxel alone ("Taxol" in top row of microscopic images shown in Fig. 2A), TRAIL alone, or paclitaxel plus TRAIL. Also, the induction by dexamethasone of either mutant p53 in Del4A or wild-type p53 in GM47.23 cells did not seem to dramatically affect the appearance of the cells after any of the three treatments (paclitaxel alone, TRAIL alone, or TRAIL with paclitaxel).

The most rigorous assessment of cellular survival after treatment is via clonogenic survival assays in which treated cells are permitted to grow undisturbed for a period of days after treatment. Clonogenic survival assays were interesting in that Del4A cells showed decreased survival after paclitaxel alone, TRAIL alone, and almost no surviving colonies after combined TRAIL and paxlitaxel. There were no appreciable differences between Del4A cells uninduced (*Mock*) or induced (*Dex*) for mutant p53 protein (top two rows of plates in Fig. 2B). GM47.23 uninduced for wild-type p53 protein also showed decreased clonogenic survival after either paclitaxel alone, TRAIL alone, and combined paclitaxel and TRAIL (Fig. 2B, *third row*). Interestingly, in contrast, induction of wild-type p53 in GM47.23 appeared to reduce cell death after any of the three treatments compared with uninduced cells, with the most notable protective effect shown in response to combination treatment with paclitaxel followed by TRAIL (bottom row of plates in Fig. 2B).

Cells that have lost clonogenic potential may conceivably remain viable. Therefore, to verify the lethal effects of drug treatment in the GBM cells, we generated cell lines that stably express bioluminescence when exposed to the substrate luciferin. This reaction requires an active luciferase enzyme, so to emit light the cells must be metabolically active. It has previously been established that the expressed light correlates accurately with cellular viability (21). Stably bioluminescent T98G and GM47.23 cell lines (designated "T98G-luc" and "GM47.23-luc" cells) were constructed as previously described (22). As shown in Fig. 2C (*top*),

Published OnlineFirst December 8, 2009; DOI: 10.1158/1535-7163.MCT-09-0415

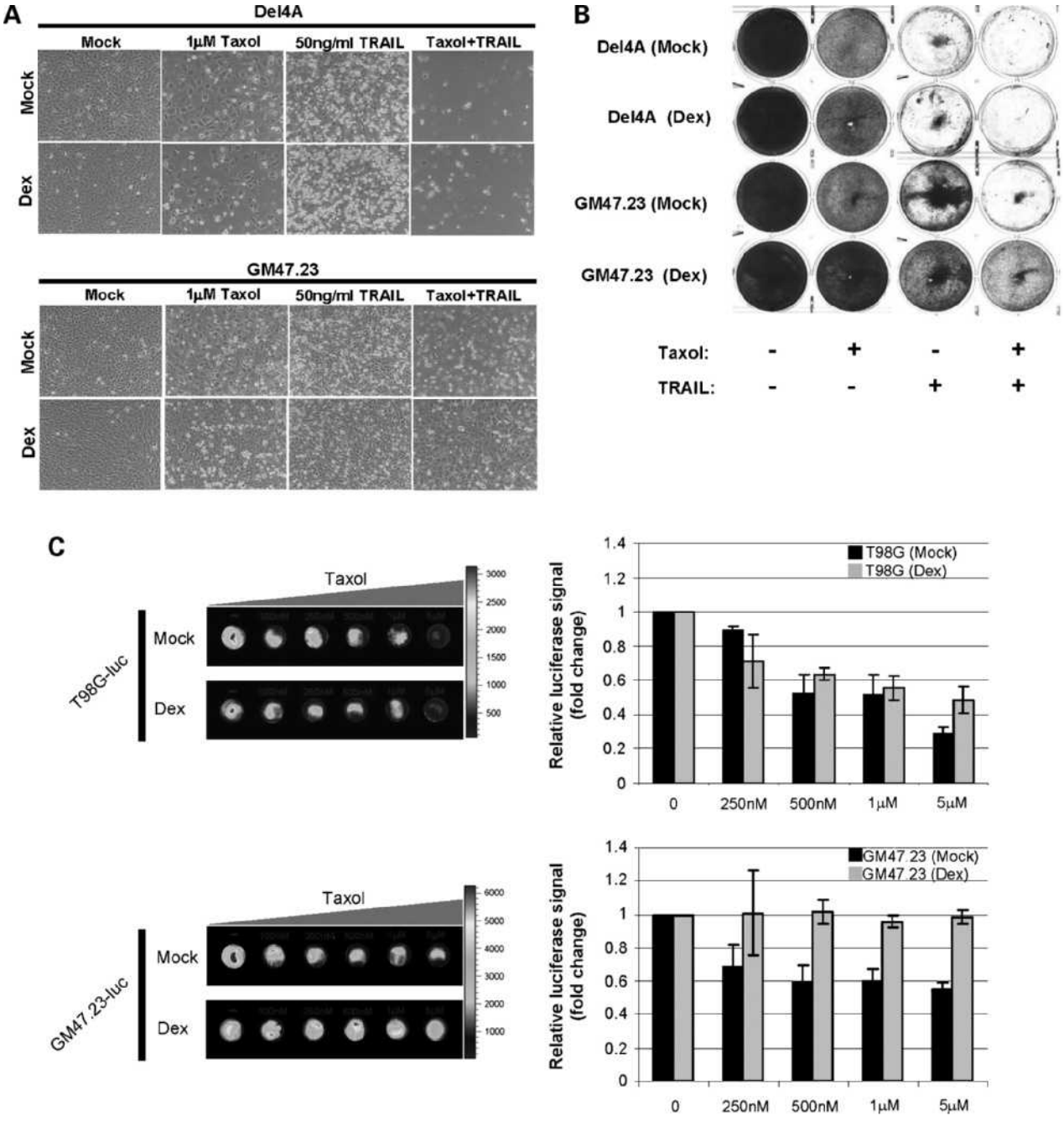

Figure 2. TRAIL augments paclitaxel-induced caspase-dependent death in glioma cells that are abrogated by induction of wild-type p53. **A** and **B,** Del4A and GM47.23 cells (1×10^6 cells/plate) were mock induced or induced with Dexamethasone (*Dex*; 1 μmol/L) as indicated for 12 h followed by sequential mock treatment or treatment with paclitaxel (1 μmol/L, 12 h) then TRAIL (50 ng/mL, additional 12 h), and then imaged with phase-contrast microscopy (**A**) or stained with Coomassie blue at 96 h (**B**). **C,** *left,* bioluminescent T98G (*T98G-luc*) and GM47.23 (*GM47.23-luc*) cells (1×10^4 cells/well) were mock induced or induced with Dexamethasone (1 μmol/L) for 12 h followed by mock treatment or treatment with paclitaxel (1 μmol/L, 12 h) and then imaged for luminescence using the Xenogen IVIS 2000 imaging platform at 5 min after addition of luciferin substrate (representative image, color scale bar represents range of signal in photons/s/cm^2/steridian). *Right,* bar graphs of median fold changes in relative luciferase signal after treatment with the indicated concentrations of paclitaxel with or without Dexamethasone induction (*columns,* mean of triplicate experiments; *bars,* SD).

T98G-luc cells were susceptible to the lethal effects of paclitaxel in a dose-dependent manner, which was not significantly affected by dexamethasone. Likewise, GM47.23-luc cells uninduced for wild-type p53 protein showed dose-dependent susceptibility to the lethal effects of paclitaxel. In contrast, induction of wild-type p53 by dexamethasone in GM47.23-luc cells was protective up to a paclitaxel concentration of 5 μmol/L (Fig. 2C, *bottom*).

Published OnlineFirst December 8, 2009; DOI: 10.1158/1535-7163.MCT-09-0415

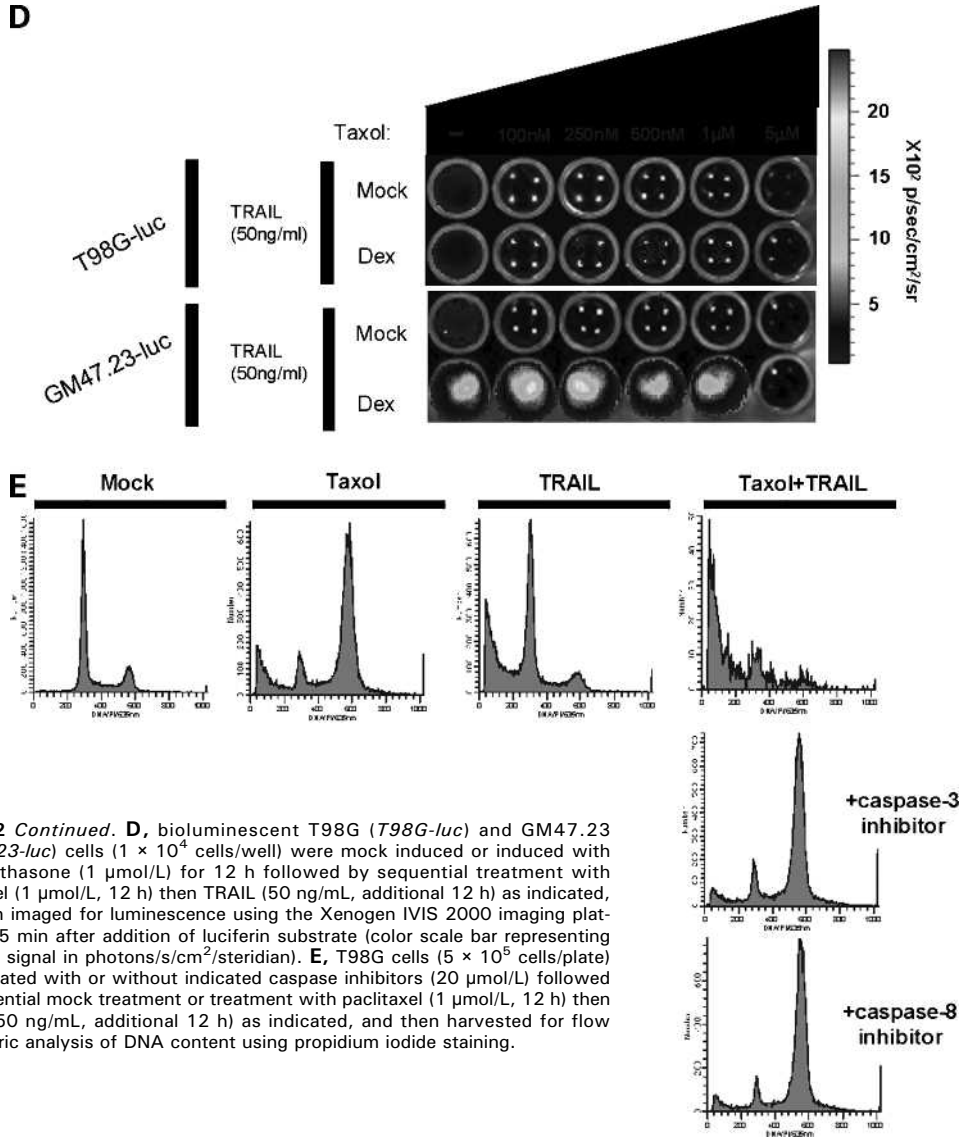

Figure 2 *Continued*. **D,** bioluminescent T98G (*T98G-luc*) and GM47.23 (*GM47.23-luc*) cells (1×10^4 cells/well) were mock induced or induced with Dexamethasone (1 μmol/L) for 12 h followed by sequential treatment with paclitaxel (1 μmol/L, 12 h) then TRAIL (50 ng/mL, additional 12 h) as indicated, and then imaged for luminescence using the Xenogen IVIS 2000 imaging platform at 5 min after addition of luciferin substrate (color scale bar representing range of signal in photons/s/cm^2/steridian). **E,** T98G cells (5×10^5 cells/plate) were treated with or without indicated caspase inhibitors (20 μmol/L) followed by sequential mock treatment or treatment with paclitaxel (1 μmol/L, 12 h) then TRAIL (50 ng/mL, additional 12 h) as indicated, and then harvested for flow cytometric analysis of DNA content using propidium iodide staining.

We next studied the effects of combined TRAIL and paclitaxel on T98G-luc and GM47.23-luc cells. Extending the previous findings, the sequential addition of TRAIL was profound when added to paclitaxel (Fig. 2D). In this experiment, the drug exposure was designed to be longer. Consequently, by the end of the experiments, there were virtually no surviving T98G-luc or GM47.23-luc cells at the highest concentration of paclitaxel (5 μmol/L) when combined with TRAIL. In the T98G-luc cells, TRAIL added to any concentration of paclitaxel resulted in almost complete cell death, regardless of the presence or absence of dexamethasone. TRAIL likewise resulted in complete cell death of GM47.23-luc cells that were uninduced for wild-type p53 at all dose levels of paclitaxel. Strikingly, induced expression of wild-type p53 in the GM47.23-luc cells led to substantially enhanced survival at concentrations of paclitaxel up to 5 μmol/L with TRAIL (Fig. 2D, *bottom, bottom set of wells*). There was no significant protective effect of dexamethasone on T98G-luc cells (Fig. 2D, *top, bottom set of wells*) as assessed with bioluminescence. These observations together are consistent with our previous observation that TRAIL markedly sensitizes cancer cells to paclitaxel (9), but intriguingly also suggest that the effects of paclitaxel and TRAIL in GBM cells may be attenuated when wild-type p53 protein is expressed.

Finally, we conducted flow cytometric analysis of T98G cells exposed to the individual or combination therapies. Paclitaxel or TRAIL treatment alone led to moderately increased sub-G_1 DNA content compared with mock-treated cells (Fig. 2E). Essentially, all cells showed nuclei with sub-G_1 DNA content after treatment with paclitaxel and TRAIL (Fig. 2E), suggesting an at least cooperative lethal effect of this combined treatment. Strikingly, pretreatment with either a caspase-3 or caspase-8 inhibitor prevented the majority of DNA fragmentation and cell killing in the paclitaxel plus TRAIL treatment group, suggesting a caspase-dependent mechanism of cell death. Together,

Published OnlineFirst December 8, 2009; DOI: 10.1158/1535-7163.MCT-09-0415

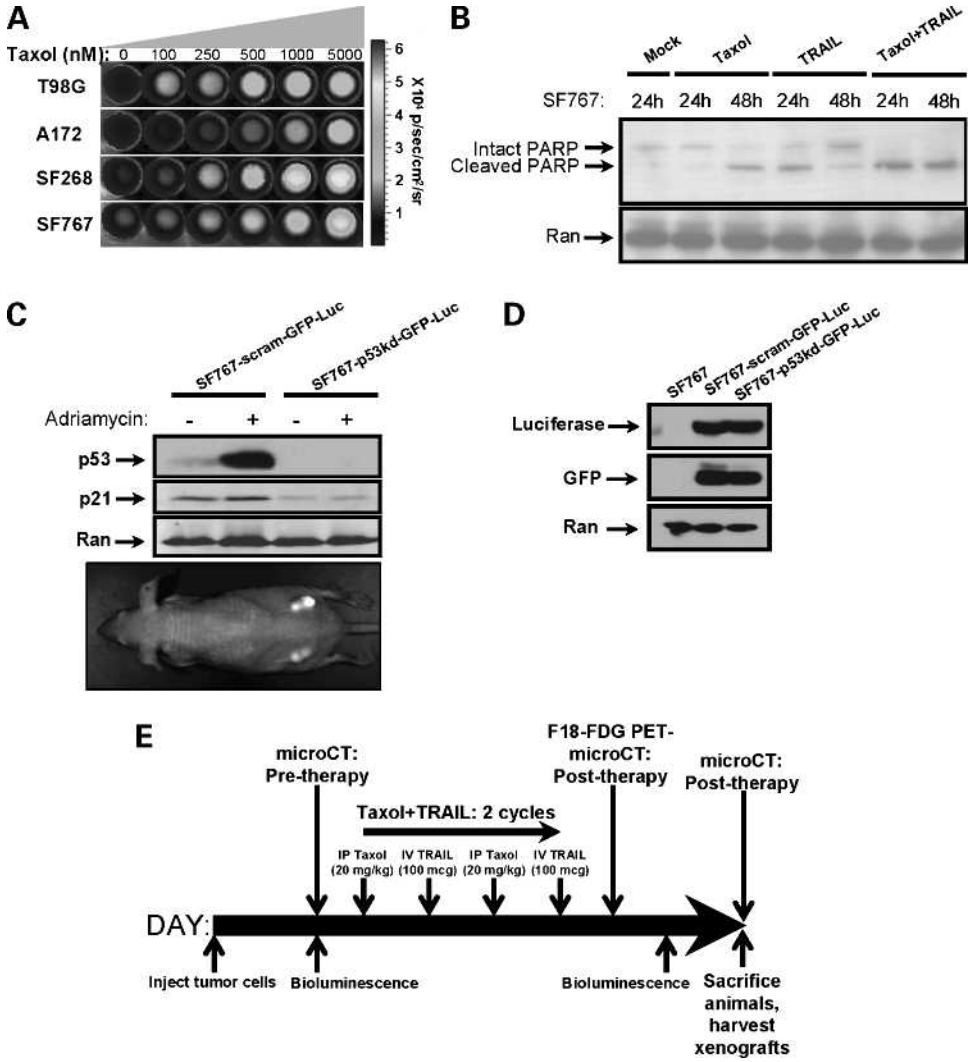

Figure 3. SF767-derived multimodality imaging glioma cell line and corresponding *in vivo* treatment schedule. **A,** GBM cell lines (T98G, A172, SF268, SF767, 1 × 10^4 cells/well) were treated with indicated concentration of paclitaxel for 12 h, processed using the Caspase-Glo 3/7 assay, and imaged with the Xenogen IVIS 2000 imaging platform. **B,** SF767 cells (1 × 10^6 cells/plate) were mock treated for 24 h or treated with paclitaxel (1 μmol/L), TRAIL (50 ng/mL), or sequential paclitaxel and TRAIL for 24 or 48 h as indicated, then harvested for Western blotting of PARP and Ran. **C,** *top,* stable SF767 cell lines coexpressing GFP and firefly luciferase and scrambled (SF767-scram-GFP-Luc) or p53 shRNA (SF767-p53kd-GFP-Luc) were treated with Adriamycin (1 μg/mL, 12 h), then harvested for Western blotting of p53, p21, and Ran as indicated. *Bottom,* representative xenograft engraftment in nude mouse by day 14 after injection of 3 × 10^6 cells (SF767-scram-GFP-Luc in the left flank, SF767-p53kd-GFP-Luc in the right flank) in Matrigel, imaged using the Cambridge Research and Instrumentation Maestro *in vivo* imaging system. **D,** SF767, SF767-scram-GFP-Luc, and SF767-p53kd-GFP-Luc cells were harvested for Western blotting of luciferase, GFP, and Ran as indicated. **E,** *in vivo* treatment and imaging schedule for preclinical study: day 0 denotes day of tumor cell injection (3 × 10^6 cells). Paclitaxel treatment on days 16 and 18, and TRAIL treatments on days 17 and 19. FDG-PET was done on day 24, and microCT was done on days 14, 24, and 46. Animals were sacrificed humanely and xenografts were harvested at the completion of the study on day 47.

these observations suggest that combined treatment with TRAIL and paclitaxel is associated with caspase activation and effective cell killing that may be attenuated by induction of wild-type p53.

Combined TRAIL Plus Paclitaxel Has *In vivo* Antitumor Effects against SF767 Human GBM Tumor Xenografts

We wished to extend our investigations of the effects of TRAIL and paclitaxel into the animal, using optical imaging (e.g., based on luciferase activity). Optical imaging has become a useful surrogate measure of tumor growth and response to therapy in many recently published studies, and thus, we used this approach in our studies (23–25). Due to the inability of T98G-based cell lines to grow in the nude mice, we expanded our *in vivo* investigation to the GBM cell line SF767. SF767 cells are particularly well suited for these studies because they grow well as a xenograft and after screening a panel of human GBM cell lines, seem to have dose-dependent increases in caspase activation in response to paclitaxel treatment as assessed by the Caspase-glo 3/7 assay (Fig. 3A). In pilot studies, SF767 cells produced solid ellipsoid tumors in 100% of injected mice (n = 5; Supplementary

Published OnlineFirst December 8, 2009; DOI: 10.1158/1535-7163.MCT-09-0415

Fig. S1B; Fig. 3C, *bottom*). SF767 cells have an endogenous $p53^{WT/WT}$ genotype and showed enhanced caspase activation and cell death (as indicated by PARP cleavage in Fig. 3B and cell morphology in Supplementary Fig. S1A) when treated with paclitaxel and TRAIL. To create an isogenic experimental cell line deficient for p53, we prepared SF767 cells in which p53 was stably repressed through the expression of short hairpin RNA (shRNA) targeting p53. A counterpart cell line expressing scrambled shRNA was also prepared, which retained wild-type p53 to serve as a control (Fig. 3C, *top*). As shown in Fig. 3D, both cell lines were also engineered to express green fluorescent protein (GFP) and luciferase (*Luc*) so that the xenografted cells could be easily detected against the host mouse tissues by detection of either fluorescence or luminescence. These efforts resulted in cells we called "SF767-p53kd-GFP-Luc" (deficient for p53) and "SF767-scram-GFP-Luc" (Supplementary Fig. S1B; Fig. 3C).

SF767-p53kd-GFP-Luc (deficient for p53) and SF767-scram-GFP-Luc were injected into the flanks of nude mice, and within 14 days, tumor formation could be detected for both cell lines. The mice were then treated according to the treatment schema shown in Fig. 3E. Briefly, mice were either mock treated, treated with paclitaxel (20 mg/kg i.p.) on days 16 and 18, treated with TRAIL (100 μg i.v.) on days 17 and 19, or treated with paclitaxel (20 mg/kg i.p.) on days 16 and 18 and TRAIL (100 μg i.v.) on days 17 and 19, respectively. To use tumor bioluminescence to quantify relative xenograft growth (14), the mice were imaged using the

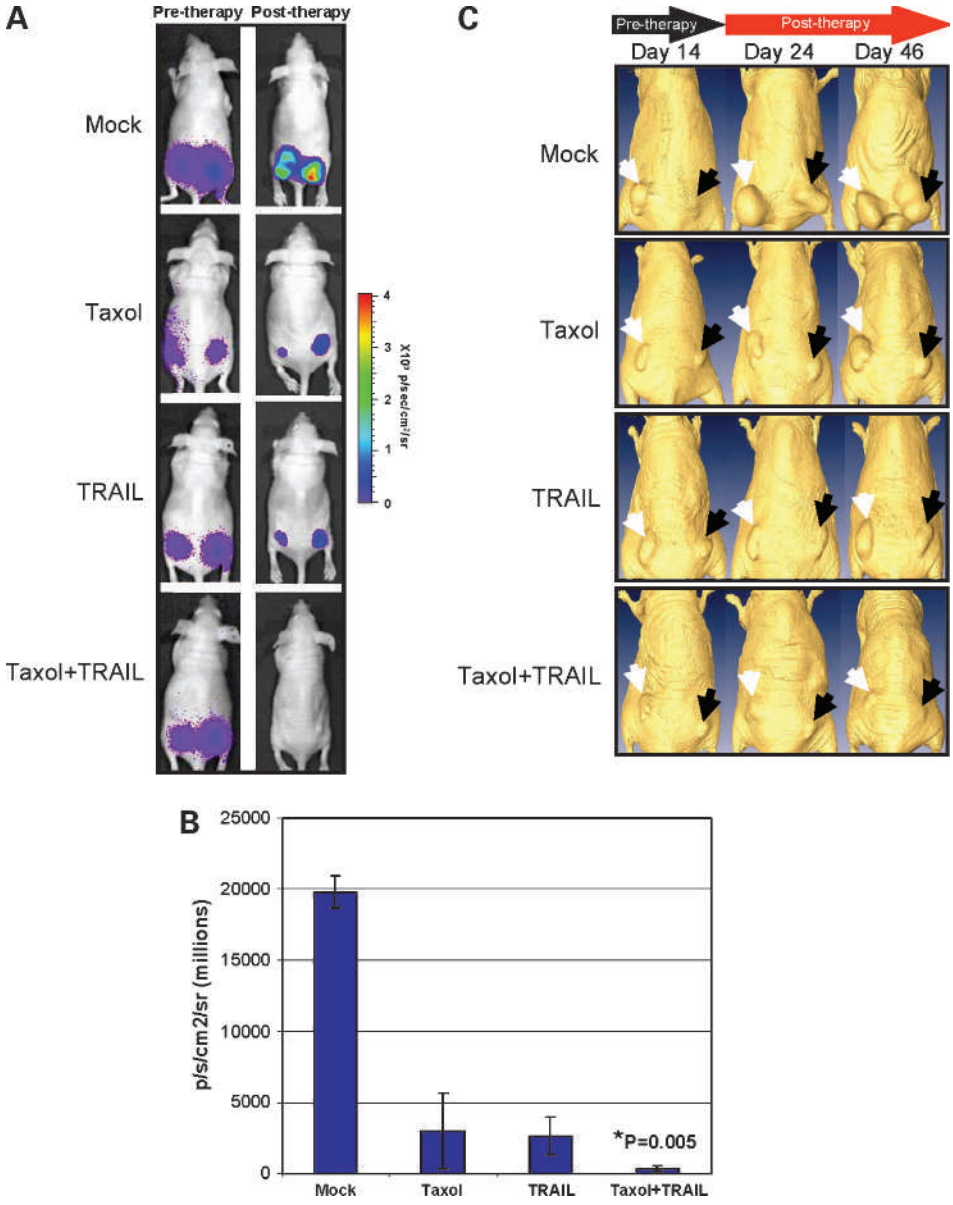

Figure 4. Combined treatment with paclitaxel and TRAIL shows efficacy *in vivo*. Luciferase-expressing SF767 tumors [SF767-scram-GFP-Luc in the left flank (*white arrows*) and SF767-p53kd-GFP-Luc in the right flank (*black arrows*)] were grown in nude mice for 14 d. Mice were either untreated (control, $n = 2$ tumors), treated with two cycles of paclitaxel (20 mg/kg i.p., days 16 and 18, $n = 2$ tumors), two cycles of TRAIL (100 μg i.v., days 17 and 19, $n = 2$ tumors), or two cycles of alternating paclitaxel and TRAIL (paclitaxel: 20 mg/kg i.p., days 16 and 18; TRAIL: 100 μg i.v., days 17 and 19, $n = 2$ tumors). **A,** mice were imaged for luciferase bioluminescence with the Xenogen IVIS 2000 on days 14 (pretherapy) and 36 (posttherapy) after i.p. injection of pharmaceutical-grade luciferin; photographs with colorwash bioluminescence overlay are shown (*color scale bar,* range of signal in photons/s/cm^2/steridian). **B,** absolute increase in median bioluminescence from day 14 to day 36 is given for each treatment cohort (*columns,* mean; *bars,* SD). *, significant difference between treatment group and mock with associated *P* value. **C,** surface reconstruction of microCTs done on mice on days 14, 24, and 46.

Published OnlineFirst December 8, 2009; DOI: 10.1158/1535-7163.MCT-09-0415

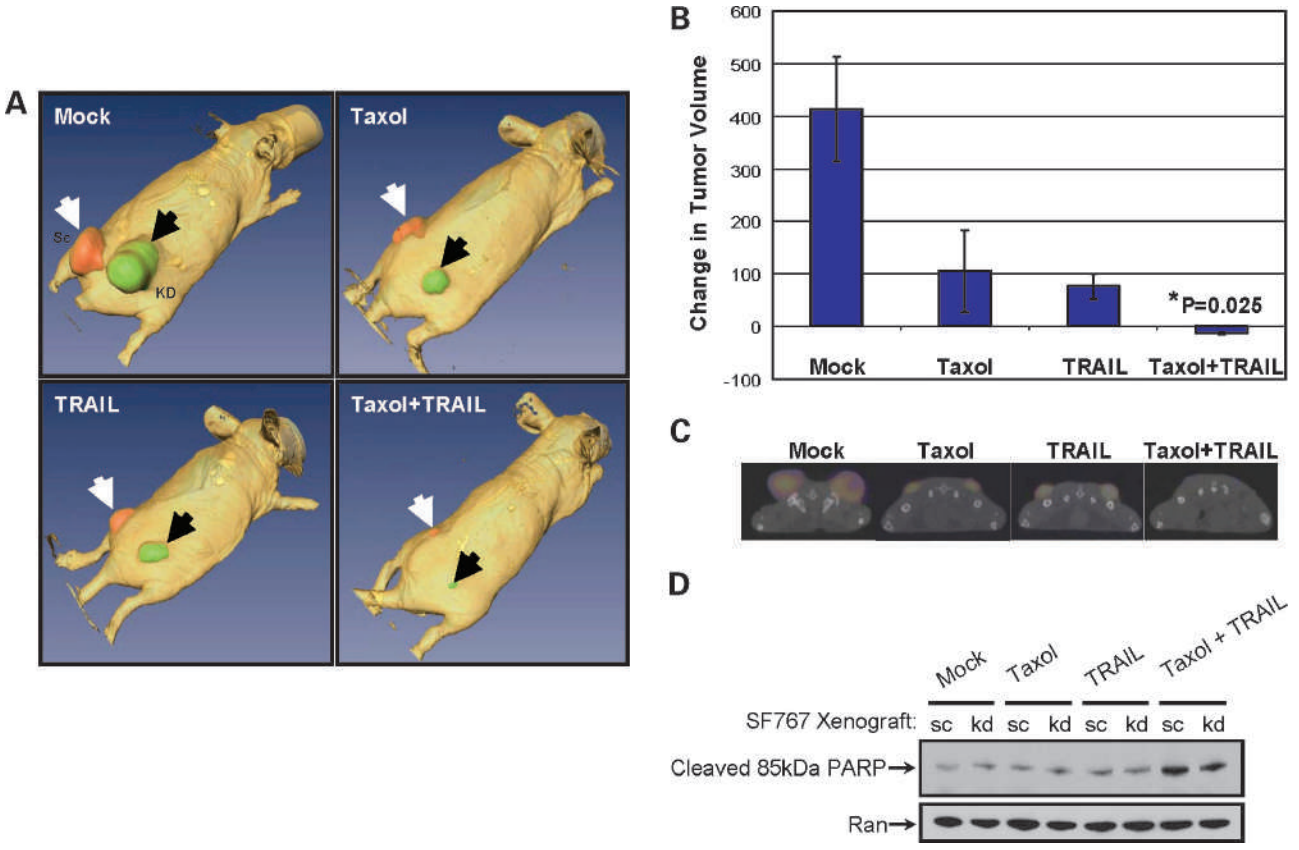

Figure 5. Combined treatment with paclitaxel and TRAIL shows efficacy *in vivo*. **A,** microCT data from day 46 were reconstructed using the Amira software. Tumor was identified, delineated slice by slice in the axial plane, and resulting tumor volumes are presented in pseudocolor (SF767-scram-GFP-Luc and SF767-p53kd-GFP-Luc in *red* and *green* pseudocolor, respectively). **B,** bar graph of tumor volume change (*columns,* mean; *bars,* SD) between treatment groups (mm^3). *, significant difference between treatment group and mock with associated *P* value. **C,** F^{18}-FDG-PET scan performed on mice on day 24 (nonspecific radiotracer uptake in the bladder and muscle was removed to improve image rendering). **D,** indicated xenografts (*sc,* SF767-scram-GFP-Luc; *kd,* SF767-p53kd-GFP-Luc) were harvested on day 47 and tumor lysate was probed after SDS-PAGE by Western blotting for analysis of cleaved PARP and Ran.

Xenogen IVIS system on days 14 (pretherapy) and 24 (post-therapy) to determine $p/s/cm^2/steridian$. As shown in Fig. 4A, all xenografts in this treatment cohort showed robust bioluminescence in pretreatment imaging. As determined by tumor bioluminescence increase after therapy, individual treatments with either paclitaxel (2.9×10^9 photons/$s/cm^2/steridian$) or TRAIL (2.6×10^9 photons/$s/cm^2/steridian$) showed tumor delay compared with control (19.8×10^9 photons/$s/cm^2/steridian$), whereas the combined treatment with paclitaxel and TRAIL had the most profound effect on suppression of bioluminescence, indicating maximal abrogation of tumor growth (3.5×10^8 photons/$s/cm^2/steridian$; Fig. 4A and B).

To verify the results derived from measurement of bioluminescence, we performed microradiographic imaging of the xenografted mice. On days 14, 24, and 47 after study initiation, the mice were imaged with microCT to volumetrically evaluate tumor progression or growth delay. As shown in Fig. 4C, untreated SF767 tumors progressed initially at a rapid rate and showed impressive size by day 46 in both p53 genetic backgrounds. Individual treatments with either paclitaxel or TRAIL resulted in some initial growth delay of tumors on day 24, and by day 46, the tumors had progressed, which is consistent with a partial response to therapy. Tumors in the combined treatment arm consisting of paclitaxel and TRAIL did not show significant tumor progression by day 46 and, of all the treatment groups, had the most profound effect on suppression of tumor growth (Fig. 4C). Tumor volume measurements were performed on axial image stacks derived from the microCTs done on days 14 and 46, and day 46 reconstructions are represented graphically after pseudocolor processing in Fig. 5A. As shown in Fig. 5B, the mock-treated tumors had an average increase in volume of 413 mm^3, whereas taxol-treated tumors and TRAIL-treated tumors had an average increase in volume of 105 mm^3 and 76 mm^3, respectively. Taxol+TRAIL-treated tumors showed minor tumor regression of 13 mm^3. Treatment with TRAIL or paclitaxel alone reduced the tumor size in both p53 knockdown and scrambled control tumors compared with mock treatment. Although TRAIL and paclitaxel showed efficacy as individual treatments, the sequential treatment of paclitaxel

Published OnlineFirst December 8, 2009; DOI: 10.1158/1535-7163.MCT-09-0415

followed by TRAIL for two cycles exhibited strong antitumor activity.

Finally, to preliminarily assess the metabolic activity in tumor xenografts, we performed PET imaging that measures the uptake of radioactive FDG, a glucose analogue (Fig. 5C). The PET scans performed posttherapy on day 24 revealed continued tumor metabolic activity above background in mock-treated control tumors, and tumors exposed to monotherapy, paclitaxel, or TRAIL. Tumors treated with combined paclitaxel and TRAIL showed no apparent increase in metabolic activity above background. Finally, xenografts were harvested to probe for PARP cleavage as an indicator of apoptosis following therapy. As shown in Fig. 5D, xenografts treated with paclitaxel and TRAIL showed increased PARP cleavage independent of p53 status when compared with either the mock-treated or monotherapy-treated (paclitaxel or TRAIL) animals.

In summary, we found the combination of TRAIL and paclitaxel profoundly repressed tumor growth in our *in vivo* studies performed in the mouse much more so than either TRAIL or paclitaxel treatment alone. These results were confirmed with assays based on imaging of bioluminescence, microradiographic imaging (microCT), and imaging of the metabolic activity of the tumors (PET). In these animal-based *in vivo* experiments, the efficient antitumor effects of combined TRAIL and paclitaxel seemed not to be influenced by the p53 status of the tumor, in contrast to the (*in vitro*) experiments with cells in culture.

Discussion

Because the majority of gliomas express both DR4 and DR5 receptors (26), the cancer cell-specific targeting properties of TRAIL make this novel biological agent an especially promising complement to traditional chemotherapies or radiation therapy. *In vivo* antitumor activities of TRAIL combined with chemotherapy or radiation have previously been reported in xenograft models of cancer including lung (27), colorectal (28), breast (29), prostate (30), and brain (31). However, the potential of combining a microtubule-targeting agent with TRAIL *in vivo* for treating glioma has apparently not been reported (6). With ongoing early clinical trials of TRAIL in various solid tumors, the issue of the degree of penetration of TRAIL through the blood-brain barrier will also need to be addressed as this is currently unknown. Nonetheless, we had previously established the *in vitro* sensitization to TRAIL by paclitaxel pretreatment in T98G glioma cells (9) and showed that paclitaxel-induced M-phase accumulation may help to "prime" cells for killing by TRAIL through cleavage of mitotic checkpoint proteins such as BubR1. Chemotherapy can theoretically sensitize tumors to TRAIL-induced apoptosis by engaging cross-talk between the intrinsic and extrinsic pathways of cell death. We sought to extend those findings here.

Mitotic checkpoints function to monitor events within M phase to assure appropriate anaphase. p53 likely intervenes subsequently in G_1 to prevent cells that have failed M phase from reinitiating replication of their DNA. Thus, rather than having a role in the spindle checkpoint of M phase, p53 functions in the G_1 phase of the cell cycle in a similar manner as in cells that have sustained either DNA damage or microtubule perturbation. Our *in vitro* studies of paclitaxel with and without TRAIL in the T98G-derived system (GM47.23, Del4A) shows a strikingly protective effect on wild-type p53–expressing cells most likely through the induction of p21 and resulting G_1 arrest. It is tempting to speculate that this effect on progression to M phase acts as a protective mechanism in normal cells with intact p53 signaling and would therefore make them less susceptible to treatment effects.

We selected the SF767 human GBM cell line to conduct our *in vivo* work because they form reproducible and well-delineated tumors in mice and display moderate sensitivity to either paclitaxel of TRAIL alone *in vitro*. However, our preliminary *in vivo* studies using stable SF767 cell lines failed to show an appreciable difference in therapeutic response between p53 wild-type and p53 shRNA knockdown tumors. In this limited preclinical study, we cannot draw any conclusions regarding our *in vivo* sensitivities to therapy across p53 genetic backgrounds. However, one can speculate that a lack of differential response could in part be attributed to the lack of robust p21 induction seen in SF767 after p53 stabilization. Furthermore, although the *p53* gene in SF767 is not deleted or mutated, other regulators of the p53 pathway may not in fact be intact and abrogate a wild-type response. Lending support to the broad antitumor effect of our treatment in both p53 genetic backgrounds in SF767 GBM tumors, there is not a great deal of correlation between therapeutic outcomes and p53 status in brain tumors (32), suggesting that in transformed cells, *p53* gene status has diminished importance compared with normal untransformed cells. This is reassuring from the standpoint of an increased therapeutic index.

Caspase activation has been implicated as the mechanism of cytotoxic action for both TRAIL and paclitaxel (33). Consistent with this view, inhibitors of caspase-3 and caspase-8 effectively block the *in vitro* ability of combined paclitaxel and TRAIL to induce cell death, indicating that these two agents likely work cooperatively through the type I intrinsic pathway for efficacy. Caspase activation has also been implicated for the *in vivo* antitumor activity of paclitaxel and TRAIL in the SF767 tumor xenograft studies. Despite the tumors being harvested weeks after the last cycle of therapy, we found that PARP cleavage was most prominent in the tumors treated with combined paclitaxel + TRAIL, regardless of the p53 background (Fig. 5D). Paclitaxel has been reported to downregulate posttranscriptionally both isoforms of FLIP protein $FLIP_S$ and $FLIP_L$, leading to apoptosis (34). SF767 xenografts tumors lacking p53 displayed a significant reduction in $FLIP_L$ after paclitaxel + TRAIL treatment, which one can speculate may have contributed in part to the striking antitumor activity (Supplementary Fig. S1C). Paclitaxel has also been reported to upregulate the DR5 receptor, potentially leading to increased binding of TRAIL to cancer cells (35). However, SF767-p53KD tumors displayed

Published OnlineFirst December 8, 2009; DOI: 10.1158/1535-7163.MCT-09-0415

decreased expression of DR5 when compared with SF767-scram with intact p53 (Supplementary Fig. S1C). This finding is in line with DR5 being a direct transcriptional target of p53 (36). We also did not find an appreciable increase in DR5 levels in p53-expressing tumors treated with paclitaxel to coincide with augmented TRAIL sensitivity (Supplementary Fig. S1C). Consistent with previous results, we found higher Mcl-1 levels in TRAIL-treated tumors (Supplementary Fig. S1C) due to transcriptional control of Mcl-1 by TRAIL (37). However, this increased Mcl-1 level did not confer significant protection against TRAIL in our current studies and may have been counteracted in part by increased phosphorylation and impairment of bcl-2.

In summary, we have shown via *in vitro* studies that combined treatment with paclitaxel and TRAIL augmented caspase-dependent human cancer cell death. *In vivo* studies confirmed that the combination treatment resulted in a remarkable antitumor effect in xenografts derived from GBM cells. To show this, we used a multimodality imaging approach including bioluminescence, microCT, and PET to assess this antitumor activity. Taken together, these studies suggest that the efficacy of chemotherapy targeting the mitotic checkpoint may be increased when administered with TRAIL. This treatment strategy warrants future preclinical investigations to confirm efficacy and further characterize the mechanism(s) of efficacy. This is particularly urgent for malignancies highly resistant to current therapies such as GBM.

Disclosure of Potential Conflicts of Interest

No potential conflicts of interest were disclosed.

References

1. Stupp R, Mason WP, van den Bent MJ, et al. Radiotherapy plus concomitant and adjuvant temozolomide for glioblastoma. N Engl J Med 2005;352:987–96.

2. Parney IF, Chang SM. Current chemotherapy for glioblastoma. Cancer J 2003;9:149–56.

3. Langer CJ, Ruffer J, Rhodes H, et al. Phase II radiation therapy oncology group trial of weekly paclitaxel and conventional external beam radiation therapy for supratentorial glioblastoma multiforme. Int J Radiat Oncol Biol Phys 2001;51:113–9.

4. Lidar Z, Mardor Y, Jonas T, et al. Convection-enhanced delivery of paclitaxel for the treatment of recurrent malignant glioma: a phase I/II clinical study. J Neurosurg 2004;100:472–9.

5. Elstad NL, Fowers KD. OncoGel (ReGel/paclitaxel)-clinical applications for a novel paclitaxel delivery system. Adv Drug Deliv Rev 2009;61:785–94.

6. Wang S, El-Deiry WS. TRAIL and apoptosis induction by TNF-family death receptors. Oncogene 2003;22:8628–33.

7. Hotte SJ, Hirte HW, Chen EX, et al. A phase 1 study of mapatumumab (fully human monoclonal antibody to TRAIL-R1) in patients with advanced solid malignancies. Clin Cancer Res 2008;14:3450–5.

8. Reardon DA, Wen PY. Therapeutic advances in the treatment of glioblastoma: rationale and potential role of targeted agents. Oncologist 2006;11:152–64.

9. Kim M, Liao J, Dowling ML, et al. TRAIL inactivates the mitotic checkpoint and potentiates death induced by microtubule-targeting agents in human cancer cells. Cancer Res 2008;68:3440–9.

10. Kim SH, Kim K, Kwagh JG, et al. Death induction by recombinant native TRAIL and its prevention by a caspase 9 inhibitor in primary human esophageal epithelial cells. J Biol Chem 2004;279:40044–52.

11. Wang S, El-Deiry WS. Requirement of p53 targets in chemosensitization of colonic carcinoma to death ligand therapy. Proc Natl Acad Sci U S A 2003;100:15095–100.

12. Fei P, Wang W, Kim SH, et al. Bnip3L is induced by p53 under hypoxia, and its knockdown promotes tumor growth. Cancer Cell 2004;6:597–609.

13. Wang W, El-Deiry WS. Bioluminescent molecular imaging of endogenous and exogenous p53-mediated transcription *in vitro* and *in vivo* using an HCT116 human colon carcinoma xenograft model. Cancer Biol Ther 2003;2:196–202.

14. Plastaras JP, Kim SH, Liu YY, et al. Cell cycle dependent and schedule-dependent antitumor effects of sorafenib combined with radiation. Cancer Res 2007;67:9443–54.

15. Wang S, Mintz A, Mochizuki K, et al. Multimodality optical imaging and 18F-FDG uptake in wild-type p53-containing and p53-null human colon tumor xenografts. Cancer Biol Ther 2007;6:1649–53.

16. Burns TF, Fei P, Scata KA, Dicker DT, El-Deiry WS. Silencing of the novel p53 target gene Snk/Plk2 leads to mitotic catastrophe in paclitaxel (taxol)-exposed cells. Mol Cell Biol 2003;23:5556–71.

17. Park CM, Park MJ, Kwak HJ, et al. Induction of p53-mediated apoptosis and recovery of chemosensitivity through p53 transduction in human glioblastoma cells by cisplatin. Int J Oncol 2006;28:119–25.

18. Blough MD, Zlatescu MC, Cairncross JG. O6-methylguanine-DNA methyltransferase regulation by p53 in astrocytic cells. Cancer Res 2007;67:580–4.

19. Lin D, Shields MT, Ullrich SJ, Appella E, Mercer WE. Growth arrest induced by wild-type p53 protein blocks cells prior to or near the restriction point in late G_1 phase. Proc Natl Acad Sci U S A 1992;89:9210–4.

20. Mercer WE, Shields MT, Lin D, Appella E, Ullrich SJ. Growth suppression induced by wild-type p53 protein is accompanied by selective down-regulation of proliferating-cell nuclear antigen expression. Proc Natl Acad Sci U S A 1991;88:1958–62.

21. Sheikh AY, Lin SA, Cao F, et al. Molecular imaging of bone marrow mononuclear cell homing and engraftment in ischemic myocardium. Stem Cells 2007;25:2677–84.

22. Wang S, El-Deiry WS. Inducible silencing of KILLER/DR5 *in vivo* promotes bioluminescent colon tumor xenograft growth and confers resistance to chemotherapeutic agent 5-fluorouracil. Cancer Res 2004;64:6666–72.

23. Szentirmai O, Baker CH, Lin N, et al. Noninvasive bioluminescence imaging of luciferase expressing intracranial U87 xenografts: correlation with magnetic resonance imaging determined tumor volume and longitudinal use in assessing tumor growth and antiangiogenic treatment effect. Neurosurgery 2006;58:365–72; discussion-72.

24. Wang W, Kim SH, El-Deiry WS. Small-molecule modulators of p53 family signaling and antitumor effects in p53-deficient human colon tumor xenografts. Proc Natl Acad Sci U S A 2006;103:11003–8.

25. Tsuruta Y, Pereboeva L, Breidenbach M, et al. A fiber-modified mesothelin promoter-based conditionally replicating adenovirus for treatment of ovarian cancer. Clin Cancer Res 2008;14:3582–8.

26. Rieger J, Naumann U, Glaser T, Ashkenazi A, Weller M. APO2 ligand: a novel lethal weapon against malignant glioma? FEBS Lett 1998;427:124–8.

27. Jin H, Yang R, Fong S, et al. Apo2 ligand/tumor necrosis factor-related apoptosis-inducing ligand cooperates with chemotherapy to inhibit orthotopic lung tumor growth and improve survival. Cancer Res 2004;64:4900–5.

28. Naka T, Sugamura K, Hylander BL, Widmer MB, Rustum YM, Repasky EA. Effects of tumor necrosis factor-related apoptosis-inducing ligand alone and in combination with chemotherapeutic agents on patients' colon tumors grown in SCID mice. Cancer Res 2002;62:5800–6.

29. Chinnaiyan AM, Prasad U, Shankar S, et al. Combined effect of tumor necrosis factor-related apoptosis-inducing ligand and ionizing radiation in breast cancer therapy. Proc Natl Acad Sci U S A 2000;97:1754–9.

30. Ray S, Almasan A. Apoptosis induction in prostate cancer cells and xenografts by combined treatment with Apo2 ligand/tumor necrosis factor-related apoptosis-inducing ligand and CPT-11. Cancer Res 2003;63:4713–23.

31. Fiveash JB, Gillespie GY, Oliver PG, Zhou T, Belenky ML, Buchsbaum DJ. Enhancement of glioma radiotherapy and chemotherapy response

Published OnlineFirst December 8, 2009; DOI: 10.1158/1535-7163.MCT-09-0415

with targeted antibody therapy against death receptor 5. Int J Radiat Oncol Biol Phys 2008;71:507–16.

32. Houillier C, Lejeune J, Benouaich-Amiel A, et al. Prognostic impact of molecular markers in a series of 220 primary glioblastomas. Cancer 2006; 106:2218–23.

33. Milross CG, Mason KA, Hunter NR, Chung WK, Peters LJ, Milas L. Relationship of mitotic arrest and apoptosis to antitumor effect of paclitaxel. J Natl Cancer Inst 1996;88:1308–14.

34. Day TW, Najafi F, Wu CH, Safa AR. Cellular FLICE-like inhibitory protein (c-FLIP): a novel target for Taxol-induced apoptosis. Biochem Pharmacol 2006;71:1551–61.

35. Nimmanapalli R, Perkins CL, Orlando M, O'Bryan E, Nguyen D, Bhalla KN. Pretreatment with paclitaxel enhances apo-2 ligand/tumor necrosis factor-related apoptosis-inducing ligand-induced apoptosis of prostate cancer cells by inducing death receptors 4 and 5 protein levels. Cancer Res 2001;61:759–63.

36. Wu GS, Burns TF, McDonald ER, III, et al. KILLER/DR5 is a DNA damage-inducible p53-regulated death receptor gene. Nat Genet 1997; 17:141–3.

37. Ricci MS, Kim SH, Ogi K, et al. Reduction of TRAIL-induced Mcl-1 and cIAP2 by c-Myc or sorafenib sensitizes resistant human cancer cells to TRAIL-induced death. Cancer Cell 2007;12:66–80.

AACR American Association for Cancer Research

Molecular Cancer Therapeutics

Tumor necrosis factor–related apoptosis-inducing ligand (TRAIL) and paclitaxel have cooperative *in vivo* effects against glioblastoma multiforme cells

Jay F. Dorsey, Akiva Mintz, Xiaobing Tian, et al.

Mol Cancer Ther Published OnlineFirst December 8, 2009.